MANY-BODY LOCALIZATION

ENEJ ŽLEBNIK JANČIČ

Fakulteta za matematiko in fiziko Univerza v Ljubljani

An isolated quantum many-body system with intrinsic interaction, will thermalize, i.e. values of local observables will settle on their thermal equilibrium values. And while that is true for the vast majority of cases that might not be true for highly disordered systems. Despite that such behavior is well known in the case of finite sized systems, known as many-body localization, the question remains, does such state survive even in the thermodynamical limit, such that it becomes a new state of matter, whose most attractive property would be its ability to locally preserve information indefinitely.

MNOGODELČNA LOKALIZACIJA

Kvantni mnogodelčni sistem z intrinzično interakcijo bo termaliziral. To pomeni, da se pričakovane vrednosti lokalnih opazljivk ustalijo pri njihovi vrednosti v termičnem ravnovesju. Čeprav slednje velja za veliko večino kvantnih sistemov, to ni nujno res za sisteme z visoko stopnjo nereda. Kljub temu, da je takšno obnašanje, imenovano tudi mnogodelčna lokalizacija, poznano za sisteme s končnim številom delcev, pa vprašanje ostaja. Ali takšno stanje preživi tudi v termodinamski limiti in s tem postane novo stanje snovi, čigar najbolj zanimiva lastnost je njegova zmožnost ohranjanja lokalne informacije.

1. Introduction

Even without a deep understanding of thermodynamics or statistical physics, people have developed a remarkably good understanding of the *thermalization* process. One can without much thinking predict that a tea bag sunk into hot water will eventually evenly color the entire water, or that a metal spoon sunken into hot soup will, after some time, become hot in its entirety. Truly, humans have developed great intuition when it comes to predicting what will happen to most many body classical systems after long enough time, even without knowledge of statistical physics.

On the other hand, we rarely, if ever, directly interact with quantum systems since the majority of quantum effects take place at scales much smaller than our own. Hence, our intuition is not really made for the quantum world, and consequently, one can find many surprises while researching quantum systems.

When talking about the thermalization in quantum many-body systems, one most of the time refers to the values of local observables after a long enough time. It turns out that for the majority of quantum many-body systems that are sent out of equilibrium, values of local observables – evaluated in the steady-state of the system – do thermalize. This means that their long time behavior is dependent only on the energy of the initial state. One then has to ask oneself, when does that not apply? The ergodic hypothesis states that after sufficiently long period of time every possible microstate of the system in a reasonable energy shell is equally probable. If we look for quantum counterparts of classical systems for which it does not apply, these are integrable systems with macroscopically many conserved quantities that do not thermalize. However, inclusion of even small perturbations can make them thermalize. Since we want a robust class of quantum many-body systems that does not thermalize under small perturbations, we turn our interest the other way. Instead of looking at the fine-tuned integrable systems, we look at the systems with high enough disorder, which could prevent thermalization.

© (2025 The Author(s). Original content from this work may be used under the terms of the Creative Commons Attribution 4.0 licence.

The systems in which our interest lies are known as local systems and have another interesting property, which is their ability to preserve information locally and indefinitely. Such property could be utilized in quantum computers and quantum informatics, where conservation of information is of vital importance.

2. Chaos: classical and quantum

Since the appearance of thermalization in a system is closely related to the presence of chaos in the system, it makes sense that understanding the dynamics of chaotic systems is a great first step toward understanding thermalization and, later, many-body localization.

2.1 Classical chaos and integrable systems

In this short chapter, we will make a quick and very simplified overview of classical chaos and integrable systems, since their quantum counterparts will play an important role in the later chapters.

It is generally agreed that a classical dynamical system is chaotic if it exhibits an exponential sensitivity of the phase-space trajectories to the small perturbations of the initial conditions. In other words, the two phase-space trajectories initially separated by distance $|\delta \mathbf{Z}_0|$ will diverge from one another at a rate $|\delta \mathbf{Z}(t)| \approx e^{\lambda t} |\delta \mathbf{Z}_0|$, where λ represents a Lyanpunov exponent.

On the other hand, there exists a class of dynamical systems that do not exhibit chaotic motion, which are known as integrable systems. Let us consider a classical Hamiltonian $H(\mathbf{p}, \mathbf{q})$ where $\mathbf{p} = (p_1, \ldots, p_N)$ represent the canonical momentum and $\mathbf{q} = (q_0, \ldots, q_N)$ represents the canonical coordinates. If such system has as many independent conserved quantities $\mathbf{I} = (I_1, \ldots, I_N)$, as degrees of freedom N, and

$${I_j, H} = 0, \quad {I_j, I_i} = 0,$$
 (1)

where $\{f,g\}$ is a Poisson bracket, then we say that the system is integrable. One can easily show that for such systems, the phase-space trajectories do not diverge at an exponential rate.

2.2 Quantum chaos and RMT

Defining chaos in quantum systems is not as simple as one might hope. While quantum mechanics can be formulated in a phase-space language using Wigner-Weyl quantization, the notion of trajectories still cannot be formulated, due to the uncertainty principle. And even if phase-space trajectories could somehow be defined, since the Schrödinger equation is linear, one cannot have exponentially departing trajectories. Even more, the overlap of two wave functions governed by the same Hamiltonian remains constant at all times:

$$\langle \psi(t)|\phi(t)\rangle = \langle \psi|\,e^{\frac{i}{\hbar}\hat{H}}\cdot e^{-\frac{i}{\hbar}\hat{H}}\,|\phi\rangle = \langle \psi|\phi\rangle. \tag{2}$$

The theory on which the quantum chaos is build is now known as a Random Matrix Theory or RMT [1] in short. It was developed by Wigner [2], Dyson [3] and others when studying the spectra of complex nuclei. Their idea was that studying the exact energy levels of such nuclei was hopeless and that one should instead focus on the general properties of their spectra. Their second insight was that the structure of Hamiltonian matrices of such complex systems would essentially look like a random matrix if written in a non-fine-tuned basis. In general, when speaking of a matrix written in a fine-tuned basis one means a basis in which the number of nonzero off-diagonal elements is small. For example, the basis in which the matrix is diagonal is the most fine-tuned. Oppositely, a non-fine-tuned basis is a basis that has many nonzero off-diagonal elements. The latter holds true if the matrix elements are inspected in a small energy window in which level density is constant. Therefore, by studying the statistical properties of random matrices (subjected

to the same symmetry constraints as the investigated Hamiltonian), one should get insight into the statistical properties of energy spectra and eigenstates of complex quantum systems.

The main ideas of RMT (and underlying Wigner-Dyson statistics) can be understood using 2×2 Hamiltonians whose entries are random numbers sampled from a Gaussian distribution

$$\hat{H} = \begin{pmatrix} \varepsilon_1 & \frac{V}{\sqrt{2}} \\ \frac{V^*}{\sqrt{2}} & \varepsilon_2 \end{pmatrix}. \tag{3}$$

Here, the prefactor $1/\sqrt{2}$ in off-diagonal matrix elements guarantees that the Hamiltonian is invariant under basis rotations, while ε_1 , ε_2 and V are random numbers. Obtaining the eigenvalue of a 2×2 matrix is trivial, and we get

$$E_{1,2} = \frac{\varepsilon_1 + \varepsilon_2}{2} \pm \sqrt{(\varepsilon_1 + \varepsilon_2)^2 + 2|V|^2}.$$
 (4)

Our interest now shifts towards obtaining the probability distribution of the spacing between the energy levels, $P(E_1 - E_2 = s) \equiv P(s)$. For simplicity, we consider only time-reversal symmetry, and therefore $V^* = V$. Under the assumption that ε_1 , ε_2 and V in Eq. (4) are taken from a Gaussian distribution with an average of 0 and a variance of σ we can write

$$P(s) = \frac{1}{(2\pi)^{3/2}\sigma^3} \int d\varepsilon_1 \int d\varepsilon_2 \int dV \delta(\sqrt{(\varepsilon_1 + \varepsilon_2)^2 + 2V^2} - s) \exp\left(-\frac{\varepsilon_1^2 + \varepsilon_2^2 + V^2}{2\sigma^2}\right).$$
 (5)

By introducing a new variable $\xi = (\varepsilon_2 - \varepsilon_1)/\sqrt{2}$, and integrating over ε_1 , we are left with

$$P(s) = \frac{1}{2\pi\sigma^2} \int \int d\xi dV \delta(\sqrt{2\xi^2 + 2V^2} - s) \exp\left(-\frac{\xi^2 + V^2}{2\sigma^2}\right),\tag{6}$$

which can be evaluated using the polar coordinates, such that $V = r \cos(\varphi)$ and $\xi = r \sin(\varphi)$. After integration, we get

$$P(s) = \frac{s}{2\sigma^2} \exp\left(-\frac{s^2}{4\sigma^2}\right). \tag{7}$$

Level spacing distribution calculated in this section corresponds to the Gaussian orthogonal ensemble (GOE), which as we stated before, describes systems with time reversal symmetry. For completeness, we should state that there are two more important classes of such ensembles, namely the Gaussian unitary ensemble (GUE), which describes systems with no time reversal symmetry, and the Gaussian symplectic ensemble (GSE), used to describe Hamiltonians with spin-orbit coupling, which has a time-reversal symmetry but no rotational symmetry. Equation (7), also known as a Wigner surmise, can be generalized to also include GUE and GSE as

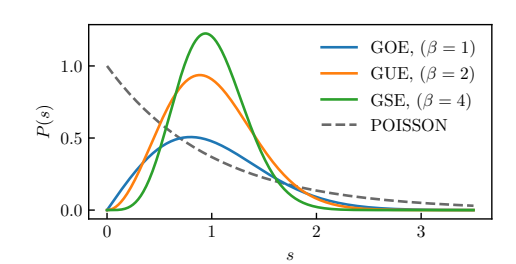


Figure 1. Level spacing distributions for the Gaussian orthogonal ensemble (GOE), the Gaussian unitary ensemble (GUE), the Gaussian symplectic ensemble (GSE) and the Poissonian ensemble.

$$P^{(\beta)}(s) = A_{\beta}s^{\beta} \exp(-B_{\beta}s^2). \tag{8}$$

Here $\beta = 1$ is used for GOE, $\beta = 2$ for GUE and $\beta = 4$ for GSE. Their distributions can be seen in Fig. (1).

For quantum systems, Wigner-Dyson distribution of level spacing signals towards the chaotic behavior. The question that remains is what would be analogy for non-ergodic systems. Example

of such systems are integrable systems, and for them, it has been shown [4] that such systems follow a Poissonian distribution

$$P_P(s) = e^{-s}. (9)$$

The statement is true for the majority of quantum systems, regardless whether they have a classical counterpart or not.

2.3 Eigenstate thermalization hypothesis

Let us consider an isolated many-body quantum system whose dynamics is governed by a Hamiltonian \hat{H} with a complete set of eigenvalues E_n and eigenvectors $|n\rangle$. If we prepare an initial state $|\psi\rangle$, that is not an eigenstate of \hat{H} , the expected value of local observable \hat{A} at time τ will be

$$A(\tau) = \sum_{m} |c_m|^2 A_{mm} + \sum_{m,n \neq m} e^{-i(E_m - E_n)\tau} c_m^* c_n A_{mn},$$
(10)

where $A_{mn} = \langle m|\hat{A}|n\rangle$ and $c_n = \langle n|\psi\rangle$. The time average of A_{τ} can then be written as [5]

$$\bar{A}(t) = \frac{1}{t} \int_0^t d\tau A(\tau) = \sum_m |c_m|^2 A_{mm} + \frac{i}{t} \sum_{m, n \neq m} e^{-i(E_m - E_n)t} \frac{c_m^* c_n}{E_m - E_n} A_{mn}, \tag{11}$$

$$\bar{A} = \lim_{t \to \infty} \bar{A}(t) = \sum_{m} |c_m|^2 A_{mm}. \tag{12}$$

We can notice that for studying long-time behavior of the observable, one should focus on properties of diagonal elements A_{mm} . Furthermore, the second term in Eq. (10) sets the timescale of approach to the equilibrium value, $\bar{A} = \lim_{t\to\infty} \bar{A}(t)$, which is determined by the properties of the off diagonal elements A_{mn} as shown in the Eq. (11). The eigenstate thermalization hypothesis (ETH) ansatz for the matrix elements of the observable in an eigenbasis of \hat{H} [6], states that for majority of systems is

$$A_{mn} = \mathcal{A}(\bar{E})\delta_{mn} + e^{-S(\bar{E})/2} f_{\mathcal{A}}(\bar{E}, \omega_{mn}) R_{mn}, \tag{13}$$

where $\bar{E} = (E_m + E_n)/2$ is the mean energy, $\omega_{mn} = E_m - E_n$ is the energy difference, R_{mn} is a random variable with a zero mean and of unit variance, $\mathcal{A}(\bar{E})$ and $f_{\mathcal{A}}(\bar{E}, \omega_{mn})$ are smooth functions and $S(\bar{E})$ is a thermodynamic entropy at an energy \bar{E} . It turns out that within the random matrix theory $\mathcal{A}(\bar{E}) = const.$ and $f_{\mathcal{A}}(\bar{E}, \omega_{mn}) = 1$. In contrast, the integrable systems do not oblige to the ansatz introduced in Eq. (13).

If we expand Eq. (12) around the mean energy $E_0 = \langle \psi | \hat{H} | \psi \rangle$ with a sufficiently small energy variance ΔE in the initial state $|\psi\rangle$, it has been shown [7] that we get

$$\lim_{t \to \infty} \bar{\mathcal{A}}(t) = \frac{1}{\mathcal{N}_{E_0, \Delta E}} \sum_{m} A_{mm} \equiv \text{Tr}[\hat{\rho}_{MC} \hat{A}]; \quad |E_0 - E_m| < \Delta E, \tag{14}$$

where $\hat{\rho}_{MC}$ represents the density of states in the microcanonical ensemble, and $\mathcal{N}_{E_0,\Delta E}$ is the number of states.

The eigenstate thermalization hypothesis also suggests that quantum thermalization greatly differs from its classical counterpart, since in the classical systems, a thermal state is constructed from the initial state which, generally does not resemble the former. In the case of the quantum systems the thermal state is already hidden in the initial state, but due to the coherence of the eigenstates it arises only after some time has passed due to the dephasing.

3. Many-body localized state

Let us now turn our attention to the question, when does the ETH ansatz from Eq. (13) apply? It turns out there is no formal proof that would guarantee the validity of the ETH for the general case, even more so for the fine-tuned integrable Hamiltonians that are counterexamples to ETH. However, our interest does not lie in such systems, since even a small perturbation could break the integrability of the system, causing it to adhere to the prediction made by the ETH.

3.1 Anderson model

A historically important model that breaks ETH is the Anderson model, which exhibits Anderson localization [8] and has no classical counterpart. One should note that the Anderson model is the quadratic model and as such does not exhibit many-body localization in which our interest lies. Nevertheless, it was shown that Anderson insulator breaks single-particle eigenstate thermalization [9].

Let's now take a bit closer look at the Anderson model. Consider N sites on a lattice where a non-interacting particle moves (in the case of the Anderson insulator, that is an electron). The Hamiltonian of such system is

$$\hat{H} = \sum_{\langle i,j \rangle} (\hat{c}_i^{\dagger} \hat{c}_j + h.c.) + \sum_i \epsilon_i \hat{c}_i^{\dagger} \hat{c}_i, \tag{15}$$

where $\hat{c}_i^{\dagger}(\hat{c}_i)$ are fermionic creation and annihilation operators acting on site *i*. The sum over neighboring sites is denoted $\langle i, j \rangle$, and ϵ_i is the on-site energy. In the case of the Anderson model, the on-site energies ϵ_i are uncorrelated random numbers. If the variance of ϵ_i in 3-dimensional system becomes sufficiently large compared to the hopping rate (first term in Eq. (15)), the particle becomes confined in the neighborhood of its original position, and the system cannot thermalize. In the case of a 1 or 2-dimensional system, the particle localizes for any nonzero variance of ϵ_i .

3.2 Defining MBL phase

Let us now turn to many-body localized state, i.e., a state of the system where particles are localized even under the interactions between particles. For such systems, it is emphasized that they avoid thermalization [10]. Let us consider an isolated many-body system whose dynamic is governed by Hamiltonian \hat{H} . If there exists a local observable \hat{A} whose long-time average follows

$$A_{\infty} = \lim_{L \to \infty} \lim_{t \to \infty} \bar{A}(t) \neq \text{Tr}[\hat{\rho}_{MC}\hat{A}], \tag{16}$$

then the system is called non-ergodic. If such non-ergodic behavior is exhibited for a robust class of initial states and observables, then we say that the system is in the MBL phase. On the other hand, if thermalization does occur for all local observables \hat{A} , i.e., Equation (14) is satisfied, we say that the system is in an ergodic phase.

In Eq. (16), we can see that it contains a double limit of infinite time $t \to \infty$ and infinite system size $L \to \infty$. It is essential that our definition of an MBL phase contains both limits since only in that case, our definition is disparate from that of an ergodic phase.

3.3 Disordered spin chain

The paradigmatic model in studies of many-body localization is 1D disordered XXZ spin 1/2-chain whose Hamiltonian reads

$$\hat{H}_{XXZ} = \sum_{i=1}^{L} J_i \left(\hat{S}_i^x \hat{S}_{i+1}^x + \hat{S}_i^y \hat{S}_{i+1}^y + \Delta \hat{S}_i^z \hat{S}_{i+1}^z \right) + \sum_{i=1}^{L} h_i \hat{S}_i^z, \tag{17}$$

where \hat{S}_i^{α} represents spin operators $\hat{\sigma}_i^{\alpha}/2$, $\alpha \in \{x, y, z\}$, periodic boundary conditions are assumed $\hat{S}_{L+1}^{\alpha} = \hat{S}_1^{\alpha}$ and $J_i = 1$ sets the energy scale. The second term represents interaction with a random magnetic fields h_i , which are independent random variables sampled from the uniform distribution on the interval [-W, W], where W is the disorder strength. In the case of $W \to 0$, the XXZ model becomes integrable and can be solved analytically using the Bethe ansatz. Parameter Δ is usually fixed to 1, and as long as its value is of the unit order, the non-equilibrium properties of a system in the presence of a disorder W are qualitatively the same.

Studies of the XXZ model have shown that with the increasing size of disorder W, the system starts to show signatures of non-ergodicity, which can be interpreted as a transition towards the MBL phase.

It should be noted that when W goes towards 0, the XXZ model becomes integrable, which somewhat complicates studying its transition from ergodic to the MBL phase, since the ergodicity window becomes quite narrow (for W = 0 system is integrable, for small values of W the system is ergodic and for large W we get MBL regime). To solve that issue, we can introduce the third term into the Eq. (17), which introduces coupling to the next-nearest neighbor, which breaks the integrability at W = 0. This system is called $J_1 - J_2$, and its Hamiltonian is written as

$$\hat{H}_{J_1 - J_2} = H_{XXZ} + \sum_{i=1}^{L} \left(\hat{S}_i^x \hat{S}_{i+2}^x + \hat{S}_i^y \hat{S}_{i+2}^y + \Delta \hat{S}_i^z \hat{S}_{i+2}^z \right). \tag{18}$$

4. Detecting MBL state

One method used for distinguishing between ergodic and the MBL state has already been established in Sec. (2.2)), where it was shown that one can differentiate between the states by studying the level spacing distribution of a system. This, of course, is not the only method used to analyze the ergodic-MBL transition and better measure of such transition would, for example, be a quantity X as shown in Fig. (2) whose value is one for the ergodic regime and of zero for the MBL regime, with a distinctive fall between both values. In addition to our demand for the distinctive separation between the two regimes, it should be noted that while our main interest lies in the MBL phase as defined in Eq. (16), with classical computers we cannot achieve system size even remotely close to that of the thermodynamic limit. With that in mind, we would also like our quantity to be able to distinctly show what happens with increasing system size.

Let us now take a look at the aforementioned quantity X and examine it behaves at different system sizes. With

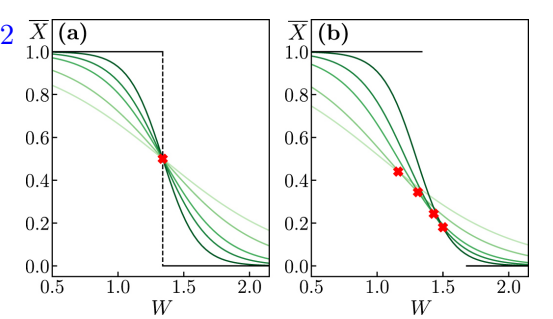


Figure 2. Here we assume that a quantity X can be used to distinguish ergodic and MBL regime. For low values of the disorder W its value is ≈ 1 which indicates that the system is in the ergodic regime, while for higher values of W its value falls towards 0. (a) Scenario in which a crossing point W^* for all system sizes is the same. (b) Scenario in which the crossing point between the consecutive system sizes is not the same. Hence, we cannot assume the stability of a MBL phase in the thermodynamic limit. Image taken from [11].

scaling of the system size, one can expect that lines representing different system sizes cross at some value of disorder W. Here, we are presented with two possible scenarios. The first scenario is that all lines representing different system sizes cross at one point W^* (here W^* denotes the crossing point for the system of a finite size, while W_C represents the transition point in the thermodynamical limit. Hence, $W^* \xrightarrow{L \to \infty} W_C$) which is shown in Fig. (2(a)). In such scenario, one can assume that even in the thermodynamical limit, the MBL regime is stable with a phase transition at $W = W_C$. The second scenario, which often arises when studying MBL, occurs when the crossing point between

consecutive system sizes starts drifting, as we can observe in Fig. (2(b)). If that is the case, system properties in the thermodynamical limit are dependent on properties of such drift, which is difficult to study with classical computers.

4.1 Gap ratio

In the case of discrete spectra of a finite-sized system, we can define the energy level spacing δ_n between adjacent energy levels as

$$\delta_n = E_{n+1} - E_n,\tag{19}$$

where the eigenvalues E_n of Hamiltonian \hat{H} are given in ascending order. We can now introduce gap ratio [12] as

$$r_n = \frac{\min\{\delta_n, \delta_{n+1}\}}{\max\{\delta_n, \delta_{n+1}\}}.$$
 (20)

In the case of a Poissonian level statistic, as shown in Eq. (9), the mean value of r_n can easily be obtained as $\bar{r}_P = 2 \ln 2 - 1 \approx 0.3863$. The mean gap ratio of the GOE can be obtained numerically, and it turns out that its mean value is $\bar{r}_{GOE} \approx 0.5307$.

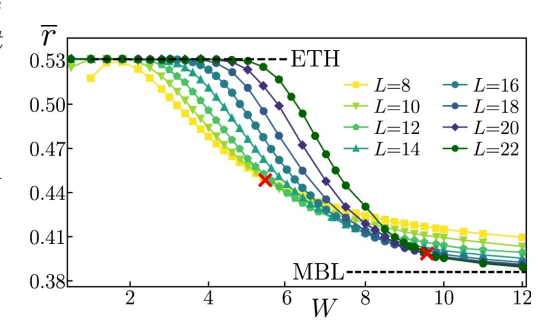


Figure 3. Average gap ratio calculated for J_1-J_2 model. Value of \bar{r} changes from $\bar{r}_{GOE}\approx 0.5307$ for small disorder W to $\bar{r}_P\approx 0.3863$ for large. Image taken from [11].

The average gap ratio calculated for the $J_1 - J_2$ model, as shown in Eq. (18) is shown in Fig. (3). We can see that for sufficiently small disorder $W \lesssim 6$ value of \bar{r} falls in order with the prediction made by the RMT, while on the other hand, for disorder strength $W \gtrsim 10$ we observe a monotonous decrease towards \bar{r}_P .

In contrast with that, we also notice a distinctive drift of W^* with scaling system size L, which could in turn be an indicator that the MBL phase in the thermodynamical limit may not survive.

4.2 Thouless time

Since the gap ratio probes the system at the smallest energy scale, namely mean level spacing $\langle \delta \rangle$, the gap ratio reflects the system's properties at the largest time scale, so-called Heisenberg time $t_H = 1/\langle \delta \rangle$, beyond which dynamics starts to become quasiperiodic. Therefore, the gap ratio is a measure applicable for probing systems at large time scales, but not so much at smaller ones.

The spectral form factor (SFF) is defined as the Fourier transform of the two-point correlation function. It provides insight into time scales much smaller than the Heisenberg time t_H . The averaged SFF can then be expressed as

$$K(\tau) = \frac{1}{Z} \left\langle \left| \sum_{j=1}^{N} g(\epsilon_j) e^{-i\epsilon_j \tau} \right|^2 \right\rangle, \tag{21}$$

where $\{\epsilon_j\}$ represents unfolded eigenvalues of a system [13], and Z is a normalization used to ensure that $K(\tau) \xrightarrow{\tau \to \infty} 1$. The filtering function $g(\epsilon)$ which is a Gaussian function with a mean in the middle of the spectrum and a variance proportional to the variance of $\{\epsilon_1, \epsilon_2, \dots, \epsilon_{\mathcal{N}}\}$ is used to reduce the effects of spectrum edges. SFF from equation Eq. (21) follows implementation from [14].

SFF can be calculated analytically for all Gaussian ensembles [1] and more specifically for GOE reads

$$K_{GOE}(\tau) = \begin{cases} 2\tau - \tau \log(2\tau - 1); & 0 < \tau \le 1\\ 2 - \tau \log(\frac{2\tau + 1}{2\tau - 1}); & \tau > 1. \end{cases}$$
(22)

 $K(\tau)$

Linear regime with logarithmic corrections for $0 < \tau \le 1$ is often referred to as the ramp, which represents long-range correlations between all pairs of eigenvalues. On the other hand, regime for $\tau > 1$ where $K_{GOE}(\tau)$ is almost constant, excluding logarithmic corrections, is called the plateau. The onset of the plateau can be interpreted as an onset of quasiperiodic dynamics beyond Heisenberg time. One should be aware that physical time of the system t and parameter τ are linked via $t = \tau t_H$.

Calculating SFF for the $J_1 - J_2$ model in the ergodic regime as shown in Fig. (4(a)) shows that for sufficiently large enough τ , SFF follows the prediction given by the GOE. The appearance of said adherence to the RMT prediction occurs at the Thouless time t_{Th} . In case of diffusive systems, the Thouless time scales quadratically

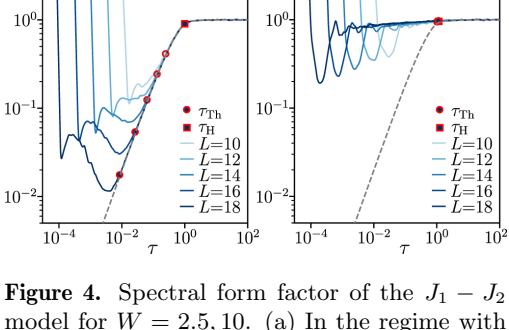
with the system size $t_{Th} \propto L^2$ [15]. The adherence of the SFF to the predictions made by RMT at the Thouless time can also be understood as an onset of quantum chaotic dynamics.

In contrast to the low disorder limit, for high enough disorder, as shown in Fig. (4), the SFF does appear to follow the Poisson level statistic $K_P(\tau) = 1$ and hence the notion of t_{Th} becomes less meaningful.

Analysis using both Heisenberg and Thouless time allows us to inspect the system at all relevant time scales. Let us now consider the ergodicity indicator g taken from [14], defined as

$$g = \log_{10}(t_H/t_{Th}) \stackrel{t_{Th} = t_H \tau_{Th}}{=} \log_{10}(1/\tau_{Th}). \tag{23}$$

Such definition of g in the thermodynamic limit interpolates between the ergodic and nonergodic regime. In ergodic regime $K(\tau)$ adheres to $K_{GOE}(\tau)$ and therefore $\tau_{Th} \to 0 \Rightarrow g \to \infty$. On the other hand in the case of nonergodic regime $K(\tau)$ adheres to $K_P(\tau)$, which approaches $K_{GOE}(\tau)$ asymptotically. From that can therefore be gathered that $\tau_{Th} \to \infty \Rightarrow g \to -\infty$. Numerical



(b) W = 10

(a) W=2.5

Figure 4. Spectral form factor of the $J_1 - J_2$ model for W = 2.5, 10. (a) In the regime with low disorder, it can be observed, that system for $\tau > t_{Th}$ adheres to $K_{GOE}(\tau)$ (dashed line). (b) In case of large disorder (MBL) phase system for large enough τ follows the result of $K_P(\tau) = 1$. Image taken from [11].

Figure 5. Ergodicity indicator g for $J_1 - J_2$ model in respect to W/L. We can see that the crossing point W^*/L is independent of the system scaling, from what, one can assume linear dependence of W^* in respect to L and from that instability of the MBL phase for $J_1 - J_2$ model. Image taken from [14].

evaluation of g for the $J_1 - J_2$ model for the system sizes $L \in \{12, 14, 16, 18\}$, as shown in Fig. (5). One can see that the crossing point W^*/L is independent of the system size L, from what could be assumed, that W^* scales linearly with respect to L as $W^*(L) = w_0 + w_1 L$ where w_0 and w_1 can be acquired using a linear fit.

Now we are left with two scenarios. First one is that a linear dependence of the W^* holds true for all system sizes. Then $W_C = W^*(L \to \infty) \to \infty$ and if that is the case, then the MBL phase is not realized in the $J_1 - J_2$ model. The second case is more optimistic and takes into account that the system sizes which are accessible to the classical computers, are far from the one of the thermodynamic limit and therefore W^* could still converge to some finite value W_C at larger systems. If that is the case, we would get a robust MBL phase.

Many-body localization

5. Conclusion

The MBL phase is still a relatively young field of research, and as such, it poses many more unanswered questions than answers. There are still uncertainties about whether our definition using the violation of a microcanonical prediction is correct and what mechanism is driving the transition from ergodic to the MBL phase, if such phase even exists. And while big steps have already been made towards answering these questions, there is still a long way ahead before we completely understand properties of the MBL phase.

REFERENCES

- [1] M. L. Mehta, Random matrices, Elsevier, 1990.
- [2] E. P. Wigner, Characteristic vectors of bordered matrices with infinite dimensions, Annals of Mathematics 62 (1955), no. 3, 548–564.
- [3] F. J. Dyson, The threefold way. algebraic structure of symmetry groups and ensembles in quantum mechanics, Journal of Mathematical Physics 3 (1962), no. 6, 1199–1215.
- [4] M. V. Berry, M. Tabor, and J. M. Ziman, Level clustering in the regular spectrum, Proceedings of the Royal Society of London. A. Mathematical and Physical Sciences 356 (1977), no. 1686, 375–394.
- [5] J. M. Deutsch, Quantum statistical mechanics in a closed system, Phys. Rev. A 43 (1991), 2046–2049.
- [6] M. Srednicki, The approach to thermal equilibrium in quantized chaotic systems, Journal of Physics A: Mathematical and General 32 (1999), no. 7, 1163.
- [7] M. Rigol, V. Dunjko, and M. Olshanii, Thermalization and its mechanism for generic isolated quantum systems, Nature 452 (2008), no. 7189, 854–858.
- [8] P. W. Anderson, Absence of diffusion in certain random lattices, Phys. Rev. 109 (1958), 1492–1505.
- [9] P. Lydžba, Y. Zhang, M. Rigol, and L. Vidmar, Single-particle eigenstate thermalization in quantum-chaotic quadratic hamiltonians, Phys. Rev. B 104 (2021).
- [10] R. Nandkishore and D. A. Huse, Many-body localization and thermalization in quantum statistical mechanics, Annual Review of Condensed Matter Physics 6 (2015), no. Volume 6, 2015, 15–38.
- [11] P. Sierant, M. Lewenstein, A. Scardicchio, L. Vidmar, and J. Zakrzewski, Many-body localization in the age of classical computing*, Reports on Progress in Physics 88 (2025), no. 2, 026502.
- [12] V. Oganesyan and D. A. Huse, Localization of interacting fermions at high temperature, Phys. Rev. B 75 (2007).
- [13] J. M. G. Gómez, R. A. Molina, A. Relaño, and J. Retamosa, Misleading signatures of quantum chaos, Phys. Rev. E 66 (2002), 036209.
- [14] J. Šuntajs, J. Bonča, T. Prosen, and L. Vidmar, Quantum chaos challenges many-body localization, Phys. Rev. E 102 (2020), 062144.
- [15] L. D'Alessio, Y. Kafri, A. Polkovnikov, and M. Rigol and, From quantum chaos and eigenstate thermalization to statistical mechanics and thermodynamics, Advances in Physics 65 (2016), no. 3, 239–362.